

Soft and joint source-channel decoding of quasi-arithmetic codes

Thomas Guionnet ^{*}; Christine Guillemot [†]

Abstract

This paper addresses the issue of robust and joint source-channel decoding of quasi-arithmetic codes. Quasi-arithmetic coding is a reduced precision and complexity implementation of arithmetic coding. This amounts to approximating the distribution of the source. The approximation of the source distribution leads to the introduction of redundancy that can be exploited for robust decoding in presence of transmission errors. Hence, this approximation controls both the trade-off between compression efficiency and complexity and at the same time the redundancy (*excess rate*) introduced by this sub-optimality. This paper provides first a state model of a quasi-arithmetic coder and decoder for binary and M -ary sources. The design of an error-resilient soft decoding algorithm follows quite naturally. The compression efficiency of quasi-arithmetic codes allows to add extra redundancy in the form of markers designed specifically to prevent de-synchronization. The algorithm is directly amenable for iterative source-channel decoding in the spirit of serial turbo codes. The coding and decoding algorithms have been tested for a wide range of channel signal-to-noise ratios. Experimental results reveal improved SER and SNR performances against Huffman and optimal arithmetic codes.

Keywords : robust arithmetic and quasi-arithmetic coding, joint source-channel coding, soft decoding, estimation, MAP.

1 Introduction

Entropy coding, producing variable length codewords (VLC), is a core component of any data compression scheme. However VLCs are very sensitive to channel noise : when some bits are altered by the channel, synchronization losses can occur at the receiver, the position of symbol boundaries are not properly estimated, leading to dramatic symbol error rates. This phenomenon has given momentum to extensive work on the design of procedures for soft decoding and joint source-channel decoding of VLCs. Soft VLC decoding ideas, exploiting residual source redundancy (the so-called “excess-rate”), have also been shown to reduce the “de-synchronization” effect as well as the residual bit and symbol error rates [23, 16, 17]. Models incorporating both VLC-encoded sources and channel codes (CC) have also been considered [15, 6, 3, 11].

The research effort has been first focused on Huffman codes [17], [15], [6], [2] and on reversible VLCs [26, 24, 3]). However, arithmetic codes have gained increased popularity in practical systems, including JPEG2000, H.264 and MPEG-4 standards. Arithmetic coding allows to decouple the coding process from the source model, hence can be used in conjunction with any probabilistic model. A good statistical model of the source is a key element to obtain maximum

^{*}All authors are with IRISA-INRIA, Campus de Beaulieu, 35042 Rennes Cedex, FRANCE. E-mail :firstname.lastname@irisa.fr

[†]Corresponding author

compression performance. However, the counterpart to the high compression efficiency is an increased sensitivity to noise : a single bit error causes the internal decoder state to be in error. Methods considered to fight against noise sensitivity consist usually in re-augmenting the redundancy of the bitstream, either by introducing an error correcting code or by inserting dedicated patterns in the chain. Along those lines, the author in [8] reintroduces redundancy in the form of parity check bits embedded into the arithmetic coding procedure. A probability interval not assigned to a symbol of the source alphabet or markers inserted at known positions in the sequence of symbols to be encoded are exploited for error detection in [4, 9, 22]. This capability can then be coupled with an ARQ procedure [5, 9] or used jointly with an error correcting code [14]. Sequential decoding of arithmetic codes is investigated in [19] for supporting error correction capabilities. The complexity of this approach is reduced in [7] by using Trellis Coded Modulation combined with a list Viterbi decoding algorithm. A soft decoding procedure is described in [10]. However, one difficulty comes from the fact that the codetree, hence the state space dimension, or number of states of the model, grows exponentially with the number of symbols being encoded. A pruning technique is then used to limit the complexity within a tractable and realistic range. However it brings inherent limitations when using the decoder in an iterative source-channel decoding structure. the pruning of the tree to limit the complexity is such that, in this particular case, the iterations do not bring a significant gain.

A fast arithmetic coding procedure, called *quasi-arithmetic coding* has been introduced in [12]. It operates on an integer interval $[0, T[$ and on integer sub-divisions of this interval. This amounts to approximate the source distribution. This controlled approximation allows to reduce the number of possible coder states without significantly degrading the compression performance. The trade-off between the state space dimension and the source distribution approximation is controlled by the parameter T . If T is sufficiently small, all state transitions and outputs can then be pre-computed and table lookups be in turn substituted for arithmetic operations. A quasi-arithmetic coder can be regarded as an arithmetic coder governed by an approximation of the real source distribution.

In this paper, we first revisit finite state automaton modeling of quasi-arithmetic coding and decoding processes for M -ary sources. Notice that the M -ary source could be coded directly with a quasi-arithmetic coder. An accurate approximation of the M -ary source distribution, would however require to set the parameter T to a high value, resulting in a high state space dimension, hence in high decoding complexity. To maintain the complexity within a tractable range, one would have to rely on a very coarse source distribution approximation. One can instead first map the M -ary source model into a binary model, by means of a fixed length binary code, represented as a binary tree with symbols at the leaves. These trees are connected up to a depth function of the source model (e.g. for an order-1 Markov source, the depth is one). Leaves of the tree represent terminated symbols, and are identified with the root of the next tree. The resulting finite binary tree can be regarded as a stochastic automaton that models the source symbol distribution. Once the M -ary source has been converted into a binary source, the latter can be encoded by a quasi-arithmetic coder. The transitions on the binary model govern the quasi-arithmetic coder. The design of an efficient estimation procedure based on the BCJR algorithm [1] follows quite naturally. The decoding complexity remains within a realistic range without the need for applying any pruning of the estimation trellis. The estimation algorithm has been validated under various channel conditions and for different levels of source correlation. Experimental results have shown very high error resilience while at the same time preserving a very good compression efficiency. For a comparable overall rate, in comparison with Huffman codes, better compression efficiency of quasi-arithmetic codes allows to dedicate extra redundan-

cy (short "soft" synchronization patterns) specifically to decoder re-synchronization, resulting in significantly higher error resilience. The usage of channel codes is also considered in order to reduce the bit error rate seen by the source estimation algorithm. The latter can then be placed in an iterative decoding structure in the spirit of serially concatenated turbo codes, provided the channel decoder and the quasi-arithmetic decoder are separated by an interleaver. Since, in contrast with optimal arithmetic coding, the estimation can be performed without pruning the trellis, the potential of the iterative decoding structure can be fully exploited, resulting in a very low symbol error rate (significantly lower than what can be obtained with Huffman codes). Overall, the great flexibility quasi-arithmetic codes offer for adjusting compression efficiency, error resilience and complexity, allows an optimal adaptation to various transmission conditions and terminal capability requirements.

The rest of the paper is organized as follows. Section 2 describes the notation we use and states the problem addressed. Sections 3 and 4 review the principles of arithmetic and quasi-arithmetic coding. Sections 5 and 6 address modeling issues of respectively coding/decoding processes and of the source. This material is exploited in the sequel (sections 7 and 8) for explaining the estimation algorithm and the "soft" synchronization procedure. Section 9 outlines the construction of the iterative joint source-channel decoding procedure based on quasi-arithmetic codes. Finally, experimental results are described in section 10. We first compare the performance of the algorithm in terms of symbol error rate (SER) and SNR with respect to soft Huffman and arithmetic decoding with theoretical Gauss-Markov sources. Simulations results of the joint source-channel turbo decoding algorithm in comparison with soft decoding of quasi-arithmetic codes are also provided.

2 Notations and problem statement

Let $A = A_1 \dots A_L$ be a sequence of quantized source symbols taking their values in a finite alphabet \mathcal{A} composed of $M = 2^q$ symbols, $\mathcal{A} = \{a_1, a_2, \dots, a_i, \dots, a_M\}$. The sequence $A = A_1 \dots A_L$ is assumed to form an order-one Markov chain. This sequence of M -ary symbols is converted into a sequence of binary symbols $S = S_1 \dots S_K$, where $K = q \times L$. This binary source is in turn coded into a sequence of information bits $U = U_1 \dots U_N$, by means of a quasi-arithmetic coder as depicted in Fig. 1. The length N of the information bit stream is a random variable, function of S , hence in turn of A . The bitstream U is sent over a memoryless channel and received as measurements Y ; so the problem we address consists in estimating A given the observed values y . Notice that we reserve capital letters to random variables, and small letters to values of these variables. For handling ranges of variables, we use the notation $X_u^v = \{X_u, X_{u+1}, \dots, X_v\}$ or \bar{X}_I where I is the index set $\{u, u+1, \dots, v\}$.

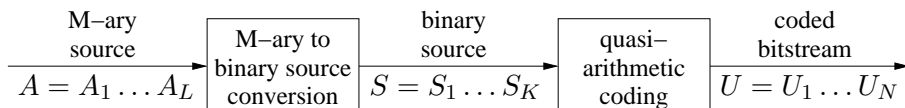


Figure 1: Conversions taking place in the coding chain.

3 Arithmetic coding principles

Let us first review the principle of arithmetic coding on a simple example of a source taking values in the alphabet $\{a_1, a_2, a_3, a_4\}$ with the stationary distribution $\mathbb{P}_a = [0.6 \ 0.2 \ 0.1 \ 0.1]$. The interval $[0, 1[$ is partitioned into four cells representing the four symbols of the alphabet. The size of each cell is the stationary probability of the corresponding symbol. The partition (hence the bounds of the different segments) of the unit interval is given by the cumulative stationary probability of the alphabet symbols. The interval corresponding to the first symbol to be encoded is chosen. It becomes the current interval and is again partitioned into different segments. The bounds of the resulting segments are driven by the model of the source. Considering an order one Markov chain, these bounds will be governed by $\mathbb{P}(A_{l+1}|A_l)$, hence in this particular case, will be function of both the probability of the previous symbol and of the cumulative probability of the alphabet symbols. Therefore, the arithmetic coder adapts in this case to the entropy *rate* $H(A_{l+1}|A_l)$ of process A , i.e. it compresses the innovation of the Markov chain A .

In the example above, when the sequence a_1, a_4, a_2, a_1 has been encoded, the current interval is $[0.576, 0.5832[$. Any number in this interval can be used to identify the sequence. Let us consider 0.576. The decoding of the sequence is performed by reproducing the coder behavior. First the interval $[0, 1[$ is partitioned according to the cumulative probability of the source. Since the value 0.576 belongs to the interval $[0, 0.6[$, it is clear that the first symbol encoded has been a_1 . Therefore the first symbol is decoded and the interval $[0, 0.6[$ is partitioned according to the cumulative probability of the source. The process is repeated until full decoding of the sequence. Practical implementations of arithmetic coding have been first introduced in [20] and [18], and developed further in [21]. One problem that may arise when implementing arithmetic coding is the high precision needed to represent very small real numbers. In order to overcome this difficulty, one can base the algorithm on the binary representation of real numbers in the interval $[0, 1[$ [25]. Any number in the interval $[0, 0.5[$ will have its first bit equal to 0, while any number in the interval $[0.5, 1[$ will have its first bit equal to 1. Therefore, during the encoding process, as soon as the current interval is entirely under or over $\frac{1}{2}$, the corresponding bit is emitted, and the interval length is doubled. There is a specific treatment for the intervals straddling $\frac{1}{2}$. When the current interval straddles $\frac{1}{2}$ and is in $[0.25, 0.75[$, it cannot be identified by a unique bit. Its size is therefore doubled, without emitting any bit, and the number of re-scaling operations taking place before emitting any bit is memorized. When reaching an interval for which one bit $U_i = u_i$ can be emitted, then this bit will be followed by a number of bits $U_{i+1} = u_{i+1} \dots U_{i+n} = u_{i+1}$, where n is the number of scaling operations that have been performed before the emission of U_i , and where $u_{i+1} = u_i + 1 \pmod 2$. The use of this technique guarantees that the current interval always satisfies $low < 0.25 < 0.5 \leq high$ or $low < 0.5 < 0.75 \leq high$, where *low* and *high* are respectively the lower and upper bounds of the current interval. This avoids the problems of precision which may otherwise occur in the case of small intervals straddling the middle of the segment $[0, 1[$.

4 Fast reduced precision implementation

Arithmetic coding is near optimality in terms of compression. Error resilient decoding solutions can be designed [10], however their complexity can be an issue in some contexts. The coding process can indeed be modeled under the form of a stochastic automaton, where the states are defined by three variables : *low*, *up* denoting the bounds of the subinterval resulting from successive sub-divisions of the interval $[0, 1[$ and n_{scl} denoting the number of scalings performed

since the last emitted bit, as explained in section 3. Subdivisions of the interval $[low, up]$, hence next states are function of the cumulative probability distribution of the source. Without the source model, the possible number of sub-divisions, hence of states, may be infinite. If the source distribution is known, the number of states still grows exponentially with the number of symbols being encoded.

4.1 Quasi-arithmetic coding

It is observed in [12] that controlled approximations can reduce the number of possible states without significantly degrading compression performance. All state transitions and outputs can then be pre-computed and table lookups can be used instead of arithmetic operations. This fast, but reduced precision, implementation of arithmetic coding is called *quasi-arithmetic coding* [12]. Instead of using the real interval $[0, 1[$, quasi-arithmetic coding is performed on an integer interval $[0, T[$. The value of T controls the trade-off between complexity and compression efficiency: if T is sufficiently large, then the interval sub-divisions will follow closely the distribution of the source. In contrast, if T is small, all the interval sub-divisions can be pre-computed.

Given the M -symbol alphabet \mathcal{A} , the sequence of symbols A_1^L is translated into a sequence of bits U_1^N by an M -ary decision tree. This tree can be regarded as an automaton that models the bitstream distribution. The encoding of a symbol determines the choice of a vertex, or branch in the tree. Each node of the tree identifies a state X of the arithmetic coder and to each transition can be associated the emission of a sequence of bits of variable length. Successive branching on the tree (or transitions between states) follow the distribution of the source ($\mathbb{P}(A_l|A_{l-1})$ for an order one Markov source, or $\mathbb{P}(A_l)$ in the zero-th order case). Let X_l denote the state of the automaton at each symbol instant l . As in the case of optimal arithmetic coding, the state X_l of the quasi-arithmetic coder is defined by three variables : $lowA_l$, upA_l and $nscl_l$. The terms $lowA_l$ and upA_l denote the bounds of the subinterval resulting from successive sub-divisions of the interval $[0, T[$ triggered by the encoding of the sequence A_1^l . The quantity $nscl_l$ is (re)-set to zero when a bit is emitted and incremented each time a re-scaling takes place. Hence, this quantity denotes the number of scalings performed since the last emitted bit. When a bit is emitted, it is followed by $nscl_l$ bits of opposite value (see section 3).

Since there is a finite number of possible integer sub-divisions of the interval $[0, T[$, all the possible states of the quasi-arithmetic coder can be pre-computed without knowledge of the source. This is however without accounting for the variable $nscl_l$. Indeed, the variable $nscl_l$ is not bounded. The solution is then to consider $nscl_l$ as a variable resulting from state transitions (output variable) and not to consider this variable in the pre-computation of the coder states. Tab. 1 gives the states, outputs and all possible transitions of a quasi-arithmetic coder pre-computed for a binary source with $T = 4$. The value of the variable $nscl_l$ is not considered in this state model. Only the action of incrementing this variable when a re-scaling is taking place is signalled by the letter f in the table, also referred to as *follow up* in [13]. The coder has three states corresponding to integer sub-divisions of the interval $[0, 4[$. The sub-divisions that can possibly take place next are function of the source probability distribution. They are chosen in such a way that the corresponding distribution approximation will minimize the excess rate [13]. For example, let us assume that the automaton is in state $X_l = 1$ (defined by the interval $[lowA_l, upA_l[= [0, 3[$). Depending on the probability of the input binary symbol 0, the interval $[0, 3[$ will be further sub-divided into $[0, 2[$, corresponding to an approximated probability of $\frac{2}{3}$, if its probability is higher than $\frac{1}{2}$, or into $[0, 1[$, corresponding to an approximated probability of $\frac{1}{3}$, if its probability is lower than $\frac{1}{2}$. Both sub-divisions result, after appropriate bit emission

and scaling, into the state 0. The number of possible states X_l is $\frac{3T^2}{16}$. If we take into account the different source distributions, the number of possible *transitions* from all the states X_l is $\frac{9T^3}{64} - \frac{6T^2}{32} + \frac{T}{4}$.

				normal state model				simplified state model			
state	$[lowA_l,$	$\mathbb{P}(0)$, corresponding		0		1		MPS		LPS	
X_l	$upA_l[$	interval sub-division		out	next	out	next	out	next	out	next
0 start	$[0,4[$	$0.63 \leq \mathbb{P}(0)$	$[0,3[$	-	1	11	0	-	1	11	0
		$0.37 \leq \mathbb{P}(0) < 0.63$	$[0,2[$	0	0	1	0	0	0	1	0
		$\mathbb{P}(0) < 0.37$	$[0,1[$	00	0	-	2				
1	$[0,3[$	$0.5 \leq \mathbb{P}(0)$	$[0,2[$	0	0	10	0	0	0	10	0
		$\mathbb{P}(0) < 0.5$	$[0,1[$	00	0	f	0				
2	$[1,4[$	$0.5 \leq \mathbb{P}(0)$	$[1,3[$	f	0	11	0				
		$\mathbb{P}(0) < 0.5$	$[1,2[$	01	0	1	0				

Table 1: Quasi-arithmetic coder states, transitions and outputs for $T = 4$.

The number of states can be further reduced by identifying the symbols as more probable (MPS) and less probable (LPS) rather than as 1 and 0. This amounts to reducing the number of possible combinations of the binary source probabilities, the MPS being either the symbol 0 or the symbol 1. This allows to combine transitions and eliminate states as shown in Tab. 1. The sequence $X_0 \dots X_L$ is a Markov chain and the output of the coder is function of transitions of this chain. This state representation can help designing a robust MAP decoder. For a deeper understanding of quasi-arithmetic coding, the reader may refer to [12].

4.2 Quasi-arithmetic decoding

Let us first consider the operation of an optimum arithmetic decoder. A sequence of arithmetically coded bits U_1^N is translated into a sequence of symbols A_1^L by a binary decision tree. Each bit determines the choice of a vertex in the tree. Each node ν of the tree identifies a state of the arithmetic decoder and corresponds to a tuple U_1^{n-1} from which two transitions are possible $U_n = 0$ or $U_n = 1$. The state of the decoder is specified by two intervals : $[lowU_n, upU_n[$ and $[lowA_{L_n}, upA_{L_n}[$. The interval $[lowU_n, upU_n[$ defines the segment of the interval $[0, 1[$ selected by a given input bit sequence U_1^n . The interval $[lowA_{L_n}, upA_{L_n}[$ relates to the sub-division obtained when the symbol A_{L_n} can be decoded without ambiguity. Both intervals must be scaled appropriately in order to avoid numerical precision problems. However, in contrast with the coding process, there is no need to keep track of the scalings that have been performed.

Let us now consider the interval $[0, T[$ and finite interval sub-divisions. The quasi-arithmetic decoder can also be expressed in the form of an automaton. Let X_n be its state at bit instant n . X_n stores the four variables $[lowU_n, upU_n[$ and $[lowA_{L_n}, upA_{L_n}[$. Since there is a finite number of possible sub-divisions of the interval $[0, T[$, there is a finite number of states for the quasi-arithmetic decoder which can be pre-computed. Tab. 2 gives the states, transitions and outputs of the quasi-arithmetic decoder for a binary source and $T = 4$, with the MPS/LPS simplification. The decoder in this particular example has two states. Further sub-divisions that will lead to transitions to next states, are function of the source probability distribution (e.g. $\mathbb{P}(MPS)$ in Tab. 2). Let us assume, for example, that the automaton is in state $X_n = 0$ (defined by the two intervals $[lowU_n, upU_n[= [0, 4[$ and $[lowA_{L_n}, upA_{L_n}[= [0, 4[$), and that the

input is $U_n = 0$. Depending on the probability of the source to be coded (hence here of the MPS and LPS symbols), the interval $[0, 4[$ will be further sub-divided into $[0, 3[$ (if MPS probability is higher than 0.63) or into $[0, 2[$ (if MPS probability is lower than 0.63), both sub-divisions resulting into the state 0.

state X_n	state variables	$\mathbb{P}(MPS)$ (corresponding sub-division of $[lowA_{L_n}, upA_{L_n}[$)	$U_n = 0$		$U_n = 1$	
			out	next	out	next
0 (start)	$[lowU_n, upU_n[: [0, 4[$	$0.63 \leq \mathbb{P}(MPS)$ ($[0, 3[$)	MPS, MPS	0	-	1
	$[lowA_{L_n}, upA_{L_n}[: [0, 4[$	$0.37 \leq \mathbb{P}(MPS) < 0.63$ ($[0, 2[$)	MPS	0	LPS	0
1	$[lowU_n, upU_n[: [2, 4[$ $[lowA_{L_n}, upA_{L_n}[: [0, 4[$	$0.63 \leq \mathbb{P}(MPS)$ ($[0, 3[$)	MPS, LPS	0	LPS	0

Table 2: Quasi-arithmetic decoder states, transitions and outputs for $T = 4$.

4.3 Source distribution approximation

Arithmetic coding realizes a conversion of source distributions : In the general case, it realizes a conversion of a sequence of symbols of an M -ary source of a given distribution into a sequence of symbols of a binary source with an independent and uniform distribution. A quasi-arithmetic coder does not produce a sequence of independently and uniformly distributed bits, due to the approximation of the source distribution that it realizes. It has been shown in [13] that this approximation does not induce a significant increase in code length. This however depends on the source statistics. This statement is true if the symbol probabilities are comprised between $1/t$ and $(t - 1)/t$, where t is the width of the current interval to be sub-divided. Hence, the choice of the value of T may depend on the source distribution. The excess rate resulting from the approximation can be computed as follows. Let a be a symbol taking its value in \mathcal{A} , $\mathbb{P}(a)$ the probability of the event a , and $\mathbb{Q}(a)$ the approximation of $\mathbb{P}(a)$ made by the quasi-arithmetic coder. The entropy of the source is given by

$$H = - \sum_{a=a_1}^{a_M} \mathbb{P}(a) \log_2 \mathbb{P}(a). \quad (1)$$

The performance of the quasi-arithmetic coder can then be measured by

$$R = - \sum_{a=a_1}^{a_M} \mathbb{P}(a) \log_2 \mathbb{Q}(a). \quad (2)$$

The excess rate induced by the quasi-arithmetic coder can hence be expressed as

$$\begin{aligned} E &= R - H, \\ &= \sum_{a=a_1}^{a_M} \mathbb{P}(a) \log_2 \frac{\mathbb{P}(a)}{\mathbb{Q}(a)}, \\ &= D(P||Q), \end{aligned} \quad (3)$$

where $D(P||Q)$ is the Kullback-Leibler distance or relative entropy between the approximate distribution Q and the true distribution P .

5 Source model

For a binary source, the variable T can be limited to a small value (down to 4) at a small cost in terms of compression [13]. This motivates a conversion of the M -ary source into a binary source, to be then encoded by the quasi-arithmetic coder. This conversion amounts to a fixed length binary coding of the source.

Let us first assume that the source quantized on $M = 2^q$ symbols is an order-0 Markov source. It can then be represented by a binary tree of depth q , as shown in Fig. 2-a for $M = 4$. The transition probabilities on the binary tree can be computed easily from the distribution of the source. The resulting binary tree can be seen as an automaton that models the M -ary source stationary distribution. A complete model of the source can be obtained by connecting the *successive local models*. One possible solution consists in identifying the leafnodes of the binary tree with the rootnode of the next tree. This leads to the three states automaton of Fig. 2-b, in the particular case of an order-0 Markov source with $M = 4$. In Fig. 2-c, the same automaton is shown in the form of a trellis, with the probability of each bit indicated on the corresponding transition. Relying on this stochastic automaton model, the sequence of the resulting binary symbols can be modeled as a function of a hidden Markov model. Let C_k denote the state ν of the automaton after k binary symbols have been produced. The sequence C_0, \dots, C_K is a Markov chain, and the resulting sequence of binary symbols is a function of transitions of this chain, i.e. $S_k = \phi(C_{k-1}, C_k)$.

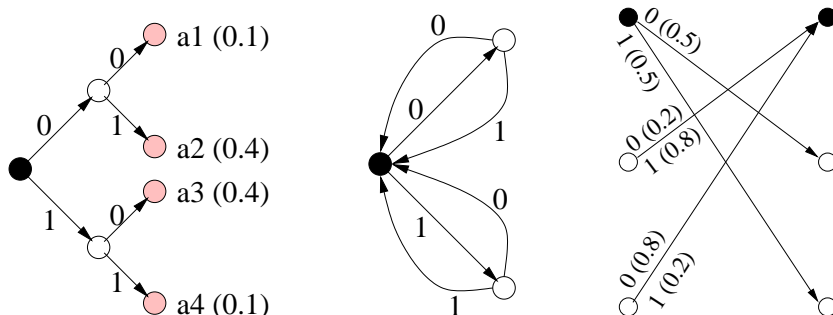


Figure 2: Graphical representation under the form of a a)-tree, b)- stochastic automaton, c)-trellis of the *binary* model of the order-0 Markov source. Black dots correspond to leafnodes identified to rootnodes of next trees. White dots correspond to intermediate nodes of the binary representation of the M -ary symbols ($M = 4$)

Let us now assume that the source is an order-1 Markov source. To take into account the correlation present in the M -ary source, in the model construction, one must in addition keep track of the last M -ary symbol coded. In order to do so, one could define the state variable C_k as a pair (ν, σ) where σ is the value of the last completed symbol A_l , and ν is the current state of the stochastic automaton describing the construction of the next M -ary symbol, following $\mathbb{P}(A_{l+1}|A_l)$. Alternately, one can take into account the conditional distribution $\mathbb{P}(A_{l+1}|A_l)$, by connecting $M + 1$ trees of depth q as shown in Fig. 3-a, and define the state variable C_k as a node ν in the resulting tree. The complete model of the source is then obtained by additional transitions from leaves to intermediate nodes as shown in Fig. 3-b. In this particular case, the model leads to a state space of dimension 15. The state space dimension for an order- n Markov source quantized on M symbols is given by $M^{n+1} - 1$. For both state models ($C_k = (\nu, \sigma)$ and

$C_k = (\nu)$, the sequence $C_1 \dots C_K$ is a Markov process, the transitions of which produce the sequence S of binary symbols.

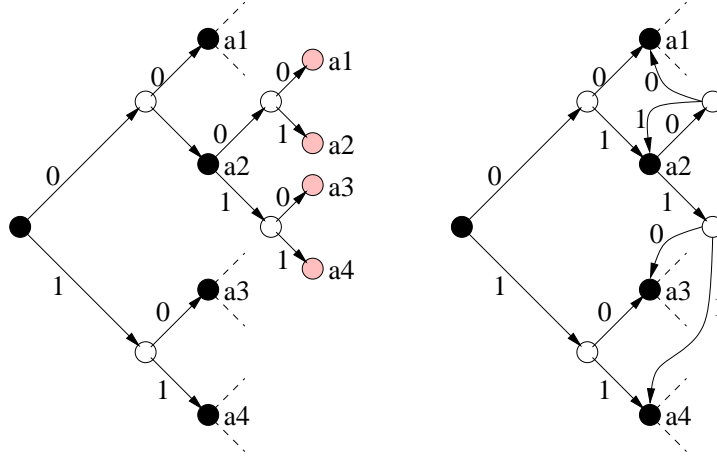


Figure 3: Graphical representation under the form of a a)-tree, b)- stochastic automaton, of the *binary* model of the order-1 Markov source. ($M = 4$)

Remark : The construction of the binary model, i.e., the assignment of the binary codewords to the different symbols has a strong impact on the reliability of the estimation. The transition probabilities on the binary tree are indeed defined by this symbol-to-leave assignment. Increased estimation reliability can be obtained when the different paths (or branches) on the model have a highly non uniform likelihood, i.e., when the uncertainty of some branches is much lower than for others. The assignment of binary codewords to symbols must hence be such that the expression $\sum_X \mathbb{P}(X)H(X)$ is minimized, where $\mathbb{P}(X)$ is the probability of the state X of the model and where $H(X)$ is the entropy of the transitions leaving X . For small source alphabets, the minimization can be achieved by a simple exhaustive search approach. However, for larger size alphabets, the exhaustive search among all possible index assignments rapidly becomes untractable. This complexity can be reduced by limiting the search space to a subset of index assignments. In the experiments reported here, this subset has been obtained by a simple circular shift of an initial index assignment. This initialization has an impact on the resulting SER and SNR performances. A lexicographic index assignment to symbols ranked by decreasing probability values turned out to provide good performance.

6 Modeling bitstream dependencies

In order to design efficient algorithms for estimating the sequence of symbols that has been emitted, one has now to build a model of bitstream dependencies. For this, we consider the *product* (in the sense of product on automata, or of tensor product of stochastic models) of the source and coder or source and decoder models. Estimation algorithms can be defined for both models. However, in section 7, the estimation is performed only on the product of the source and decoder models, since with the source and coder model, handling the $nscl_k$ variable can increase dramatically the number of states. For the source, in the sequel, we consider the *binary* source and model described in section 5.

6.1 Product model: source + coder

The state of the product system must gather state information of two automata, the automaton modeling the source distribution and the coder model. Hence, the state X_k of the product system is defined as $X_k = (lowS_k, upS_k, C_k)$. One could expect the dimension of the resulting state space to be the product of dimensions of the states spaces of the two models (source and coder). However, simplifications occur. Again, this is better explained with the simple source and coder examples of Tab. 1 and Fig. 2.

The system resulting from the product of the coder of Tab. 1 and the order-0 Markov source model of Fig. 2-c is illustrated in Fig. 4. For $T = 4$ and using the MPS/LPS simplification, the transitions do not lead to re-scalings of the interval $[lowS_k, upS_k[$. For different values of T , re-scaling of the interval could occur and would then be signaled with the same notation f as in Tab. 1. Since the coder model has 2 states and the binary source model has 3 states, the dimension of the resulting state space should in principle be 6. However, it turns out that in general fewer states are necessary (only 4 states instead of 6 in the simple coder and source examples of Tab. 1 and Fig. 2). This simplification results from the fact that the transitions in the coder model are function of the source probability distribution. Depending on the stationary probabilities of the input binary source, the general coder model given in Tab. 1 simplifies as shown in Fig. 5. The probabilities of the binary symbols resulting from the conversion of the M -ary source depend on the previous state of the source model. Therefore, transitions on the source model will trigger the use of one or the other quasi-arithmetic trellis. In the example of Fig. 5-b, it can be verified easily that some states will never be reached, hence reducing the state space dimension from 6 to 4.

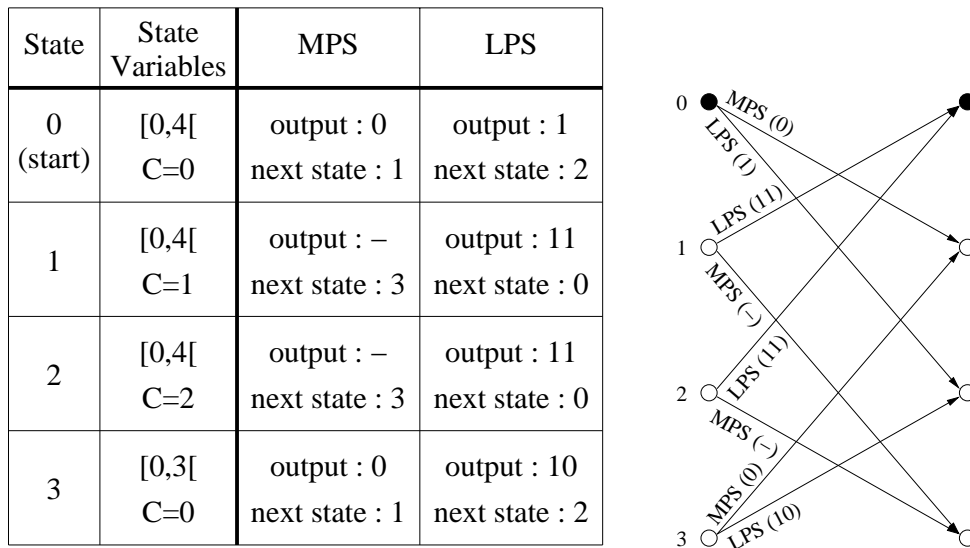


Figure 4: Source-coder product model: a) States, outputs and transitions; b) Trellis representation.

In general, the state space dimension can not be known a-priori, it must be computed given T and the binary source model. If N_C is the number of states of the binary source model, the maximum number of states is $\frac{3T^2 N_C}{16}$.

The number of bits being produced by each transition on the above model being random,

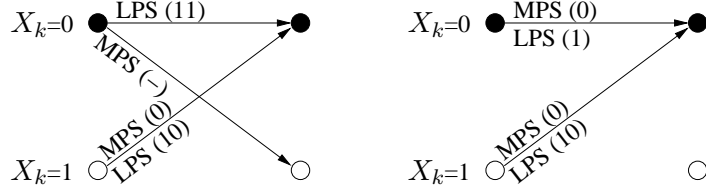


Figure 5: Quasi-arithmetic coder model: a) $0.63 \leq \mathbb{P}(MPS)$; b) $0.5 \leq \mathbb{P}(MPS) < 0.63$.

the structure of dependencies between the sequence of measurements and the model states is random. In order to capture this randomness, we actually consider the augmented Markov chain $(X, N) = (X_1, N_1) \dots (X_K, N_K)$. This yields the structure of dependencies graphically depicted in Fig. 6. Using this model, a sequence of binary symbols S_1^K is translated into a sequence of bits $U_1^{N_K}$, where N_K is the number of bits emitted when K symbols have been encoded. Given a state X_k and an input symbol S_{k+1} , the automaton specifies the bits $\bar{U}_{k+1} = U_{N_k+1}^{N_{k+1}}$ that have to be emitted and the next state X_{k+1} . Notice that no bits may be emitted by a transition. The probabilities of successive branchings (e.g. of transitions between $(X_k, N_k) = (lowS_k, upS_k, C_k, N_k)$ and $(X_{k+1}, N_{k+1}) = (lowS_{k+1}, upS_{k+1}, C_{k+1}, N_{k+1})$) in the trellis are given by the binary source model, i.e. $\mathbb{P}(C_{k+1}|C_k) = \mathbb{P}(S_{k+1}|C_k)$. Measurements \bar{Y}_k on the bits \bar{U}_k are gathered at the output of the transmission channel.

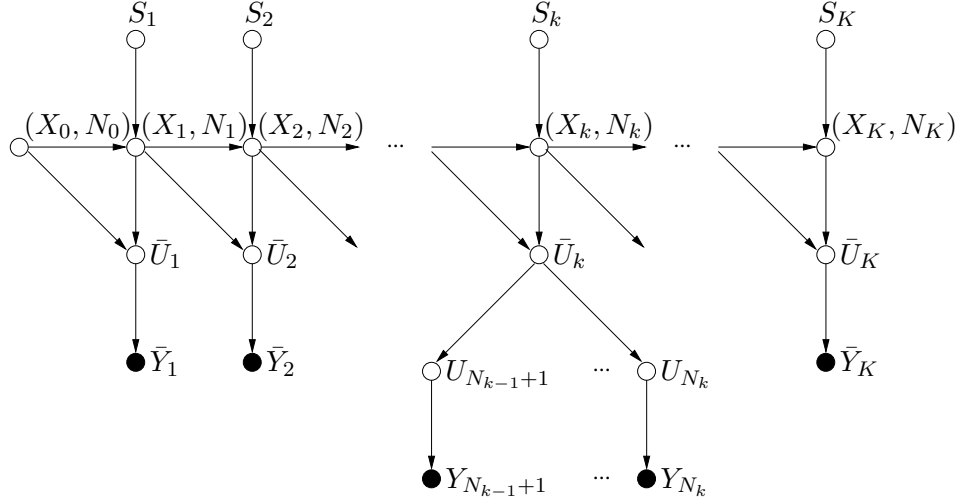


Figure 6: Source-coder product model ($N_k \geq N_{k-1}$). White and black dots represent respectively the hidden and observed variables.

6.2 Product model: source + decoder

A product model of source + decoder can be constructed similarly. The state of the product system must gather state information of the source and decoder models. Hence, the state X_n of the product system is defined as $X_n = (lowU_n, upU_n, lowS_{K_n}, upS_{K_n}, C_{K_n})$. The system resulting from the product of the decoder of Tab. 2 and the simple source model of Fig. 2-c is illustrated in Fig. 7. Again, the state space dimension depends on the coder precision parametrized by T and of the source model.

State	State Variables	0	1
0 (start)	[0,4[[0,4[C=0	output : MPS next state : 1	output : LPS next state : 2
1	[0,4[[0,4[C=1	output : MPS,MPS next state : 1	output : – next state : 3
2	[0,4[[0,4[C=2	output : MPS,MPS next state : 1	output : – next state : 4
3	[2,4[[0,4[C=1	output : MPS,LPS next state : 2	output : LPS next state : 0
4	[2,4[[0,4[C=2	output : MPS,LPS next state : 2	output : LPS next state : 0

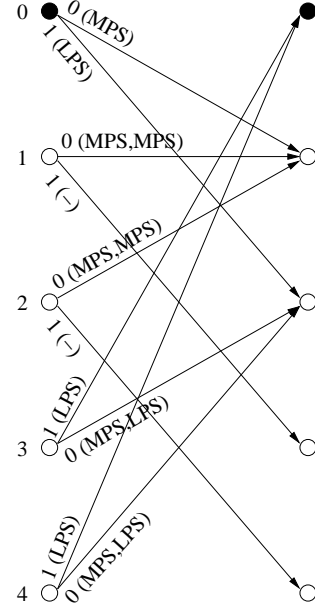


Figure 7: Source-decoder product model: a) states, outputs, transitions; b) trellis representation.

The number of symbols being produced by each transition on the above model is random. Therefore, the structure of dependencies between the sequence of measurements and the sequence of decoded symbols is random. This is handled by considering the augmented Markov chain $(X, K) = (X_1, K_1) \dots (X_N, K_N)$ with the structure of dependencies graphically depicted in Fig. 8. Using this model, a sequence of bits U_1^N is translated into a sequence of symbols $S_1^{K_N}$, where K_N is the number of symbols decoded when N bits have been received. Given a state X_n and an input bit U_{n+1} , the automaton produces the sequence of symbols $\bar{S}_{n+1} = S_{K_{n+1}}^{K_{n+1}}$ and the next state X_{n+1} . The probabilities of successive branchings (i.e. of transitions between (X_n, K_n) and (X_{n+1}, K_{n+1})) in the trellis depend on the binary source model and are given by

$$\prod_{k=K_{n+1}}^{K_{n+1}} \mathbb{P}(S_k | C_{k-1}).$$

6.3 Source distribution approximation

The entropy of the M -ary source computed on the *binary* model in section 6 (e.g. Fig.2-c) is given by

$$H(S|C) = - \sum_{c=0}^{N_C-1} \mathbb{P}(c) \sum_{s=0,1} \mathbb{P}(s|c) \log_2 \mathbb{P}(s|c), \quad (4)$$

where C denotes the state variable of the source model and c the indice of the possible values it can take. N_C is the dimension of the state space. The performance of the quasi-arithmetic coder when applied on this binary source for a given value of the parameter T can be measured

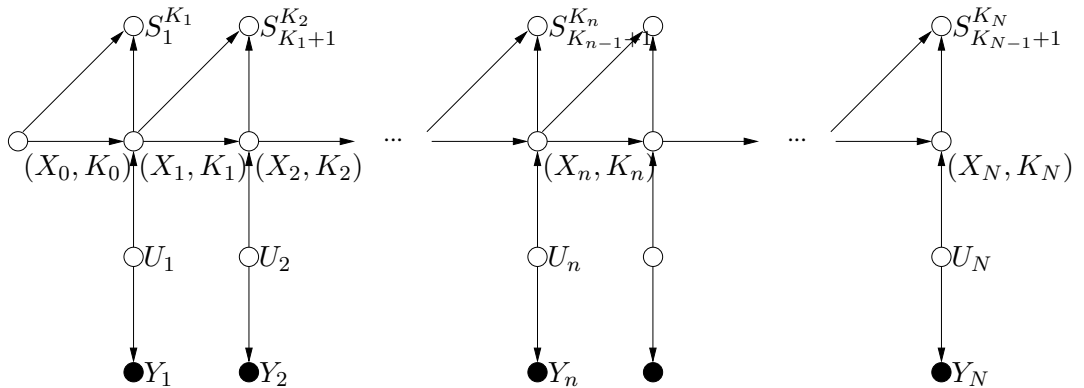


Figure 8: Source-decoder product model. White and black dots represent respectively the hidden and observed variables.

by

$$R(S|X) = - \sum_{x=0}^{N_X-1} \mathbb{P}(x) \sum_{s=0,1} \mathbb{P}(s|x) \log_2 \mathbb{Q}(s|x), \quad (5)$$

where X denotes the state variable of the product model (source + coder) and where x represents the possible indices taken by the variable X , N_X being the dimension of the state space function of T . The quasi-arithmetic coder realizes an approximation of the distribution of the *binary* source, hence of the M -ary source. This approximation is however, for a given value of the parameter T , more accurate than when applying the quasi-arithmetic coder directly on the M -ary source. Here, the excess rate, for a given value of T , is given by

$$\begin{aligned} E(S|X) &= R(S|X) - H(S|X), \\ &= \sum_{x=0}^{N_X-1} \mathbb{P}(x) \sum_{s=0,1} \mathbb{P}(s|x) \log_2 \frac{\mathbb{P}(s|x)}{\mathbb{Q}(s|x)}, \\ &= D(\mathbb{P}(s|x) || \mathbb{Q}(s|x)), \end{aligned} \quad (6)$$

where $D(\mathbb{P}(s|x) || \mathbb{Q}(s|x))$ is the conditional relative entropy between the approximate conditional distribution \mathbb{Q} and the true conditional distribution \mathbb{P} . One may notice that several states of the quasi-arithmetic coder can correspond to a given state c of the binary source model. Hence, several different approximations $\mathbb{Q}(s|x)$ of $\mathbb{P}(s|x)$ can exist (See for example the states 0 and 3 of Fig. 4). The excess rate can be considered as a measure of the bitstream redundancy.

7 Estimation algorithm

The above models of dependencies can be exploited to help the estimation of the bitstream (hence of the symbol sequence). The MAP (maximum *a posteriori*) estimation criterion corresponds to the optimal Bayesian estimation of a process X given available measurements Y :

$$\hat{X} = \arg \max_x \mathbb{P}(X = x|Y). \quad (7)$$

However, if the mean square error (MSE) is the performance measure, the MAP criterion is sub-optimal. The conditional mean or minimum MSE (MMSE) is in this case the optimal

decoder. The decoder then seeks a sequence of symbol reproductions that will minimize the expected distortion given the sequence of observations, denoted $E[D(\hat{A}, A)|Y]$. These expected distortions can be computed in a very straightforward way given the MAP estimates, provided the probability measures on the sequence of binary symbols S are converted into probability measures on the sequence of M -ary symbols A . In the section on experimental results, only the MAP estimates have been considered.

The optimization is performed over all possible *sequences* x . This applies directly to the estimation of the hidden states of the processes (X, N) (symbol clock model of source + coder) and (X, K) (bit clock model of source + decoder), given the sequence of measurements. The estimation is run on the source and decoder product model in order to avoid handling the $nscl_k$ variable.

Estimating the set of hidden states $(X, K) = (X_1, K_1) \dots (X_N, K_N)$ is equivalent to estimating the associated sequence of decoded symbols $S = S_1 \dots S_{K_1} \dots S_{K_N}$, given the measurements Y_1^N at the output of the channel. The best sequence (X, K) can be obtained from the local probabilities on the pairs (X_n, K_n) by the equation

$$\mathbb{P}(X, K|Y) = \prod_{n=1}^N \mathbb{P}(X_n, K_n|Y). \quad (8)$$

The computation of the entity $\mathbb{P}(X_n, K_n|Y)$ can be organized around the factorization

$$\mathbb{P}(X_n, K_n|Y) \propto \mathbb{P}(X_n, K_n|Y_1^n) \cdot \mathbb{P}(Y_{n+1}^N|X_n, K_n), \quad (9)$$

where \propto denotes a renormalization factor. The Markov property allows a recursive computation of both terms of the right-hand side, using the BCJR algorithm [1]. The forward sweep concerns the first term

$$\begin{aligned} \mathbb{P}(X_n = x_n, K_n = k_n|Y_1^n) &= \sum_{(x_{n-1}, k_{n-1})} \mathbb{P}(X_{n-1} = x_{n-1}, K_{n-1} = k_{n-1}|Y_1^{n-1}) \cdot \\ &\quad \mathbb{P}(X_n = x_n, K_n = k_n|X_{n-1} = x_{n-1}, K_{n-1} = k_{n-1}) \cdot \\ &\quad \mathbb{P}(U_n = u_{(x_{n-1}, k_{n-1})(x_n, k_n)}|Y_n). \end{aligned} \quad (10)$$

The terms on the right-hand side of the equation are respectively the recursive term, the transition probability given by the product model (see section 6), and the probability to have emitted the bit U_n triggering the transition between $X_{n-1} = x_{n-1}$ and $X_n = x_n$, given the measure Y_n (channel model). The process is initialized at the starting state $(0, 0)$, and allows to compute $\mathbb{P}(X_n, K_n|Y_1^n)$ for all possible states (x_n, k_n) , and for each bit clock instant $n = 1, \dots, N$.

The backward sweep provides the second term in Eqn. 9

$$\begin{aligned} \mathbb{P}(Y_{n+1}^N|X_n = x_n, K_n = k_n) &= \sum_{(x_{n+1}, k_{n+1})} \mathbb{P}(Y_{n+2}^N|X_{n+1} = x_{n+1}, K_{n+1} = k_{n+1}) \cdot \\ &\quad \mathbb{P}(X_{n+1} = x_{n+1}, K_{n+1} = k_{n+1}|X_n = x_n, K_n = k_n) \cdot \\ &\quad \mathbb{P}(U_{n+1} = u_{(x_n, k_n)(x_{n+1}, k_{n+1})}|Y_{n+1}). \end{aligned} \quad (11)$$

The process is initialized for all possible “last” states (x_N, k_N) and allows to compute $\mathbb{P}(Y_{n+1}^N|X_n, K_n)$ for all possible states (x_n, k_n) , and for each bit clock instant consecutively from N to 1.

As in [6, 16], a termination constraint can be introduced : one can ensure that the decoder produces the right number of symbols ($K_N = K$) (if known). All the paths in the trellis which

do not lead to a valid sequence length are suppressed. The trellis on which the estimation is performed can be pre-computed, with all transitions and outputs stored. Fig. 9 shows the trellis computed with the example product model of Fig. 7 for a sequence of $K = 7$ symbols producing $N = 6$ bits.

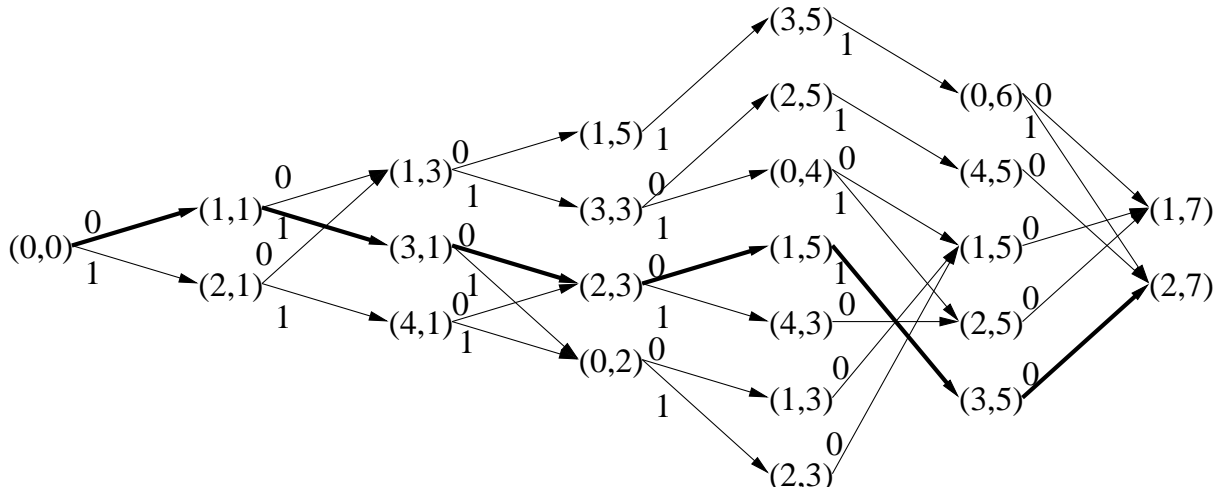


Figure 9: Example of trellis for $K = 7$, $N = 6$.

8 Soft synchronization

Termination constraints mentioned in section 7 can be regarded as means to force synchronization at the end of the sequence : they indeed constrain the decoder to have the right number of symbols ($K_N = K$) (if known) after decoding the estimated bit stream \hat{U} . These constraints ensure synchronization at the end of the bit stream, but do not ensure synchronization in the middle of the sequence. One can introduce extra information specifically to help the resynchronization “in the middle” of the sequence. For this, we consider here the introduction of extra bits at some known positions $I_s = \{i_1, \dots, i_s\}$ in the symbol stream. This extra information takes the form of dummy binary symbols (in the spirit of the techniques described in [4], [7], [19], [8] and [22]), inserted in the binary symbol stream, at some known symbol clock positions, after the conversion of the M -ary source into the binary source. Since these dummy symbols are inserted at some known symbol clock instants, the position of the corresponding extra bits in the coded bitstream depends on the sequence of symbols encoded, hence is random.

Models and algorithms above have to account for this extra information. Inserting an extra dummy symbol at known positions in the symbol stream amounts to add a section with deterministic transitions in the binary tree model of the source. The presence of this extra information can be exploited by the estimation. During the estimation process, the variable K_n indicates when a marker should be expected. The corresponding transition probabilities in the estimation trellis are updated accordingly. A null probability is given to all transitions that do not emit the expected sequence of binary symbols, while a probability of one is set to the others. Therefore, some paths in the estimation trellis become forbidden and can be suppressed, leading to a reduction of the number of states.

9 Iterative CC-AC decoding algorithm

The soft synchronization mechanism described above increases significantly the reliability of the segmentation and estimation of the sequence of symbols. One can however consider in addition the usage of an error correction code, e.g. of a systematic convolutional channel code (CC). Both codes can be concatenated in the spirit of serial turbo codes. Adopting this principle, one can therefore work on each model (quasi-arithmetic coder and channel coder) separately and design an iterative estimator, provided an interleaver is introduced between the models. The structure of dependencies between the variables involved is outlined on Fig. 10.

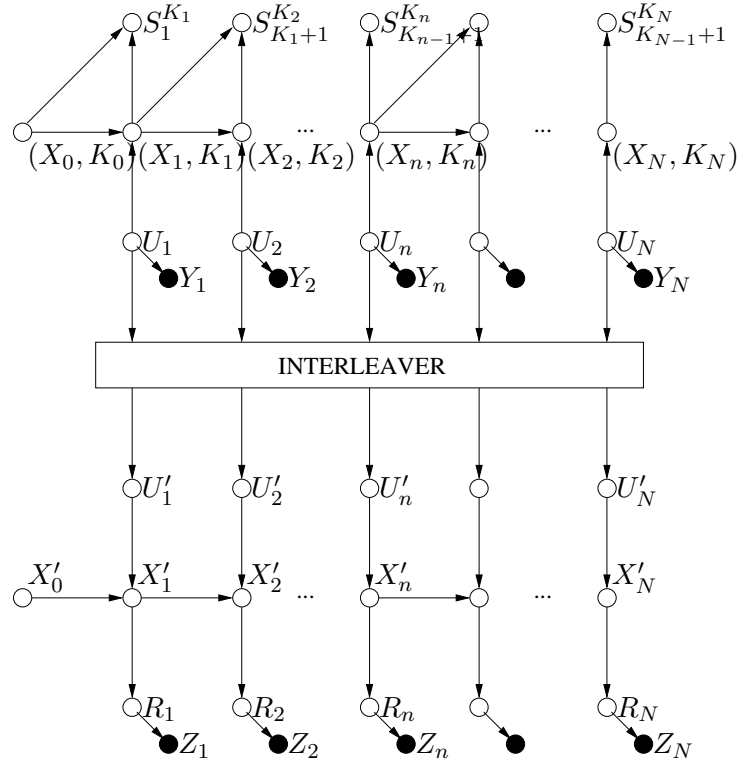


Figure 10: Graphical representation of dependencies in the joint arithmetic-channel coding chain.

Such a scheme requires extrinsic information on the bits U_n to be transmitted by the CC to the soft arithmetic decoder, and reciprocally. The extrinsic information on a bit U_n represents the modification induced by the introduction of the rest of the observations Y_1^{n-1}, Y_{n+1}^N on the conditional law of U_n given Y_n . The extrinsic information can be expressed as

$$Ext_{U_n}(Y|Y_n) \propto \frac{\mathbb{P}(U_n|Y)}{\mathbb{P}(U_n|Y_n)}. \quad (12)$$

The iterative estimation proceeds by first running a BCJR algorithm on the channel coder model. The extrinsic information on the useful bits U_n is a direct subproduct of the BCJR algorithm. These measurements can in turn be used as input for the estimation run on the quasi-arithmetic decoder model described above.

The result of the quasi-arithmetic soft decoding procedure is the a-posteriori probabilities on the states (X_n, K_n) of the estimation trellis, given the observations : $\mathbb{P}(X_n, K_n|Y)$. These a-posteriori probabilities must then be converted into extrinsic information on bits U_n . The

probability of having a bit $U_n = u_n$ given Y is the sum of the transition probabilities between all states (x_{n-1}, k_{n-1}) and (x_n, k_n) for whose this transition exists and is triggered by u_n . Thus, the a-posteriori probability of a bit U_n given the observations is obtained by the equation

$$P(U_n = u_n|Y)|_{u_n=0,1} = \sum_{(x_{n-1}, k_{n-1})} \mathbb{P}(x_{n-1}, k_{n-1}|Y) \cdot \frac{\mathbb{P}(succ_{u_n}(x_{n-1}, k_{n-1})|Y)}{\sum_{u_n=0,1} \mathbb{P}(succ_{u_n}(x_{n-1}, k_{n-1})|Y)}, \quad (13)$$

where $succ_{u_n}(x_{n-1}, k_{n-1})$ is the state (x_n, k_n) reached by the transition from (x_{n-1}, k_{n-1}) triggered by the bit $U_n = u_n$.

10 Experimental results

To evaluate the performance of the soft quasi-arithmetic decoding procedure, a set of experiments has been performed on a first-order Gauss-Markov source, with zero-mean, unit-variance and different correlation factors ρ . The source is quantized with an 8 levels uniform quantizer (3 bits) on the interval $[-3, 3]$. We consider sequences of $K = 200$ symbols with different source correlation factors. All the simulations have been performed assuming an additive white Gaussian channel with a BPSK modulation. The results are averaged over 3000 realizations.

The first experiment aimed at comparing the performances in terms of soft decoding of Huffman codes [11], arithmetic codes [10] and quasi-arithmetic codes with $T = 4$, for comparable overall rates. When the source correlation increases, the compression efficiency of the arithmetic coder increasing, soft synchronization patterns are inserted in the arithmetically encoded stream up to a comparable overall rate. Fig. 11 and 12 show the residual symbol error rates (SER) and SNR obtained for different channel E_b/N_0 , for respectively $\rho = 0.5$ and $\rho = 0.9$. For sources with low correlation ($\rho = 0.5$ and under) and for values of E_b/N_0 lower than 5 dB. (i.e. for high bit error rates), quasi-arithmetic coding outperforms both arithmetic and Huffman coding. However, for sources with high correlation, the quasi-arithmetic coder and decoder turn out to be slightly less efficient than the optimal arithmetic coder for this range of E_b/N_0 . The reason is that, excess rate induced by quasi-arithmetic coding increases with the source correlation (see section 4.3). The optimal arithmetic coding fully exploiting the source correlation, one can then insert a higher amount of "soft" synchronization patterns, for the same overall rate, resulting in an improved error resilience. The same trend has been observed for different rates. The gain brought on soft quasi-arithmetic decoding by synchronization markers is illustrated on Fig. 13 and 14, respectively for $\rho = 0.5$ and $\rho = 0.9$. Notice that, even for high correlation sources, the performances of the quasi-arithmetic decoder would obviously increase if one would allow a higher complexity, i.e. a higher value for the parameter T . In order to compare fairly the three methods, one must also consider their complexity. It can be measured by the size of the trellis used for the estimation. Considering a sequence of 200 symbols, soft decoding of Huffman codes needs two trellis with about 900 states respectively per bit clock and symbol clock instant. The complexity of soft decoding of arithmetic codes is limited to 100 states per symbol clock instant, using pruning. Finally, the soft decoding of quasi-arithmetic codes leads to a trellis containing about 2400 states per bit clock instant, hence being the most complex of the three. Pruning may be considered to reduce this complexity.

The second experiment aimed at evaluating the performance of the iterative channel/quasi-arithmetic decoding algorithm. Fig. 15 and 16 depict the SER and SNR performances, in comparison with the decoding approach with soft synchronization, respectively for $\rho = 0.5$ and $\rho = 0.9$. The first observation is that the iterations bring significant improvements, higher gain

being obtained when the source correlation is high (see Fig. 16). Nevertheless, if the source correlation is low, the soft synchronization outperforms the iterative scheme. In this range of channel signal to noise ratios, the channel code cannot correct all the errors, and the de-synchronization phenomenon prevails. It is therefore preferable to dedicate redundancy within the source to fight against these de-synchronizations. In contrast, when the source correlation is high ($\rho = 0.9$), the SER is lower with the iterative solution due to a proper exploitation of the inter-symbol correlation for segmenting and estimating the bit stream. It can also be observed that the gain brought by the iterations depends on the degree of redundancy present on both sides of the interleaver. Fig. 17 and 18 show the performances obtained when combining synchronization markers and channel coding, respectively for $\rho = 0.5$ and $\rho = 0.9$. Three approaches are compared, with equal or sufficiently close overall rates. In the first one, only channel coding ($k/n = 2/3$ and 4 iterations) is used to add redundancy. In the second one, channel coding ($k/n = 5/6$ and 4 iterations) is combined with synchronization markers. Finally, in the third approach, only synchronization markers are used. For sources with high correlation, channel coding leads to higher performance, since the correlation present in the source is already exploited efficiently to fight against desynchronizations. For sources with low correlation and for values of E_b/N_0 lower than 3 dB., on the contrary, the combination of channel coding and synchronization markers has been found to be the best strategy. It has also been observed that, in this case, iterations bring a higher gain than in other cases.

In another set of experiments, the influence of the length of the sequence on the system performance is considered. Fig. 19 and 20 depict the SER and SNR performances with three different lengths, respectively for $\rho = 0.5$ and $\rho = 0.9$. As expected, the performance decreases when the length of the sequence increases. This can be explained by the exploitation of the termination constraint which contributes to the decoder resynchronization. The length of the sequence has also an influence on the complexity of the decoding. Indeed, this complexity depends on the size of the estimation trellis, which depends mainly on the *excursion*, i.e. the possible values, of the variable K_n . The excursion is higher in the middle than at the extremities of the sequence. Hence, it reaches higher values with longer sequences. We have measured experimentally the average number of states of the trellis per bit clock instant n . The values obtained are 557, 1177 and 2376 respectively for sequences of 50, 100 and 200 symbols. Pruning techniques may be required for longer sequences.

In the last experiment, the impact of the precision of the quasi-arithmetic coder parameterized by the variable T has been analyzed. Fig. 21 provides the SER and SNR performances for $T = 4$ and $T = 8$ without extra redundancy, and for $T = 8$ with soft synchronization patterns added to obtain a bit rate comparable to the case where $T = 4$ ($\rho = 0.5$). The lower precision coder ($T = 4$) due to the presence of residual redundancy is more resilient to errors. However, the coder with a higher precision ($T = 8$) allows, by better exploiting the source statistics, to obtain higher compression efficiency and in turn dedicate redundancy to re-synchronize the decoding process. Then the overall performances appear to be similar for E_b/N_0 larger than 4 dB. Once again, the complexity is an issue. Indeed, increasing the value of T leads necessarily to a higher number of states. In this experiment, we have found the following average number of states of the estimation trellis per bit clock instant : 1193 when $T = 4$, 4736 when $T = 8$ and 4297 when $T = 8$ with the insertion of synchronization markers. Therefore, it is highly desirable to choose T as small as possible.

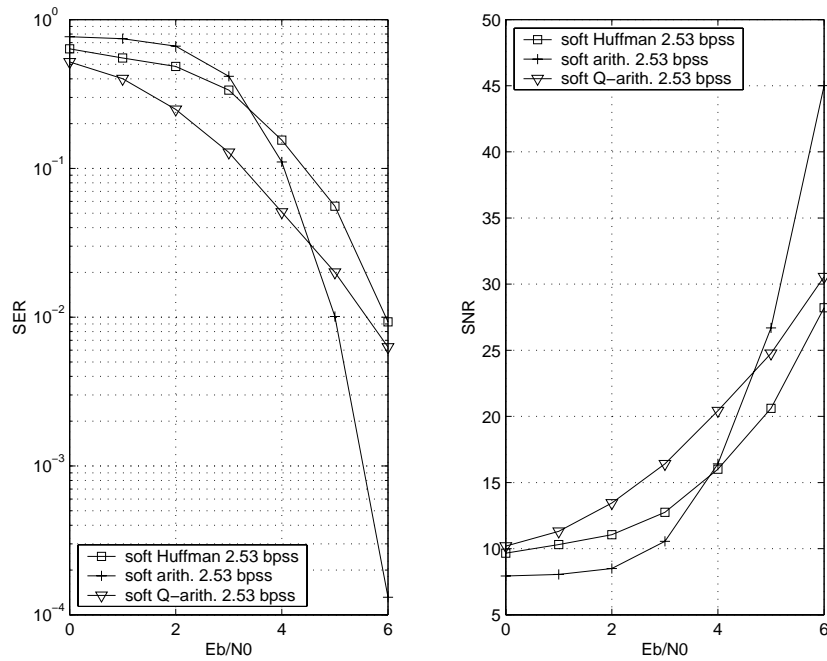


Figure 11: SER and SNR performances of (a) soft Huffman decoding (b) soft arithmetic decoding and (c) soft quasi-arithmetic decoding ($\rho = 0.5$, 200 symbols, 3000 channel realizations).

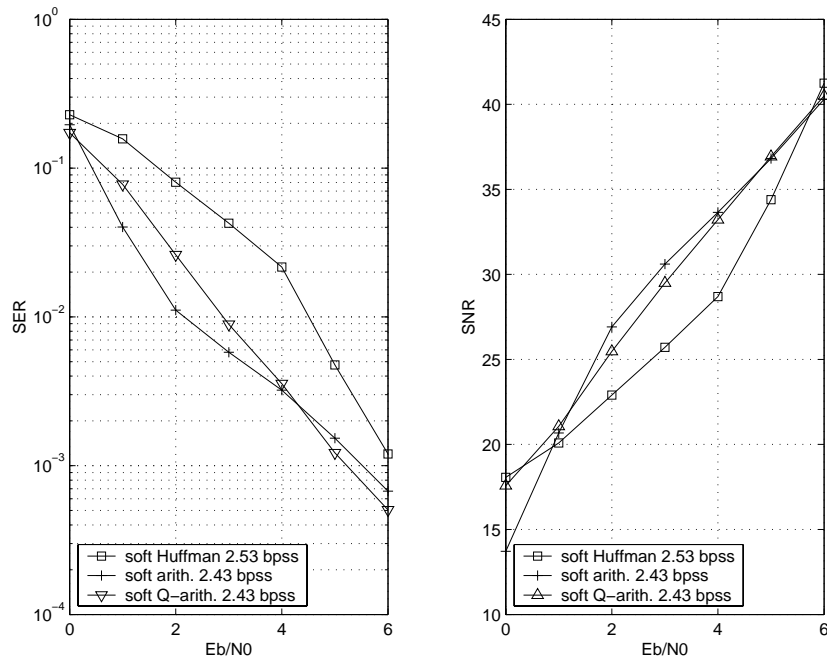


Figure 12: SER and SNR performances of (a) soft Huffman decoding (b) soft arithmetic decoding and (c) soft quasi-arithmetic decoding ($\rho = 0.9$, 200 symbols, 3000 channel realizations).

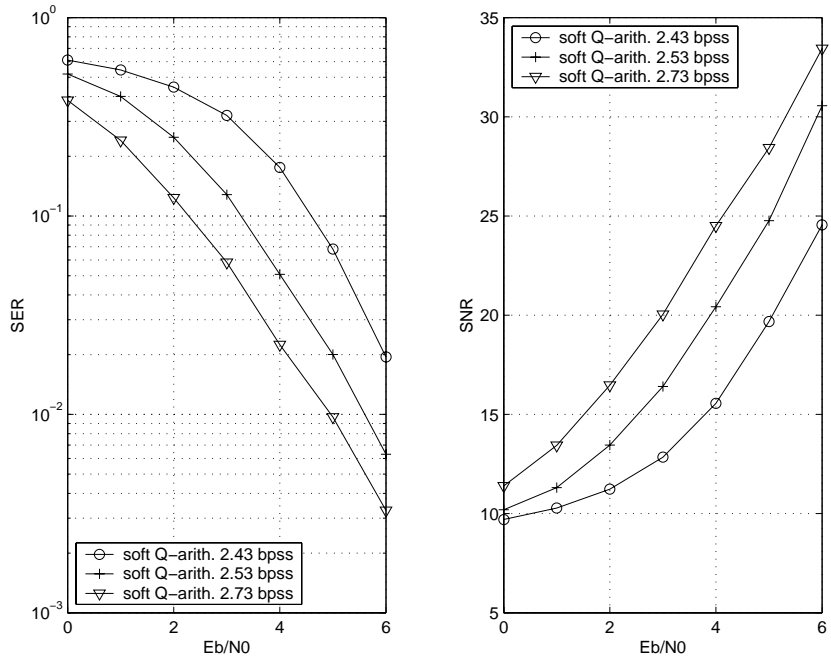


Figure 13: SER and SNR performances of soft quasi-arithmetic decoding for different rates ($\rho = 0.5$, 200 symbols, 3000 channel realizations).

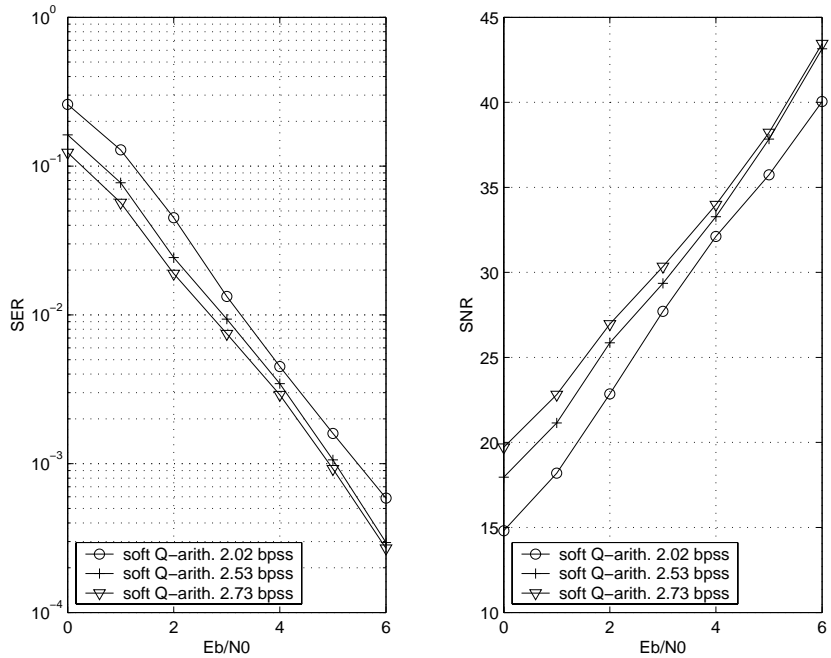


Figure 14: SER and SNR performances of soft quasi-arithmetic decoding for different rates ($\rho = 0.9$, 200 symbols, 3000 channel realizations).

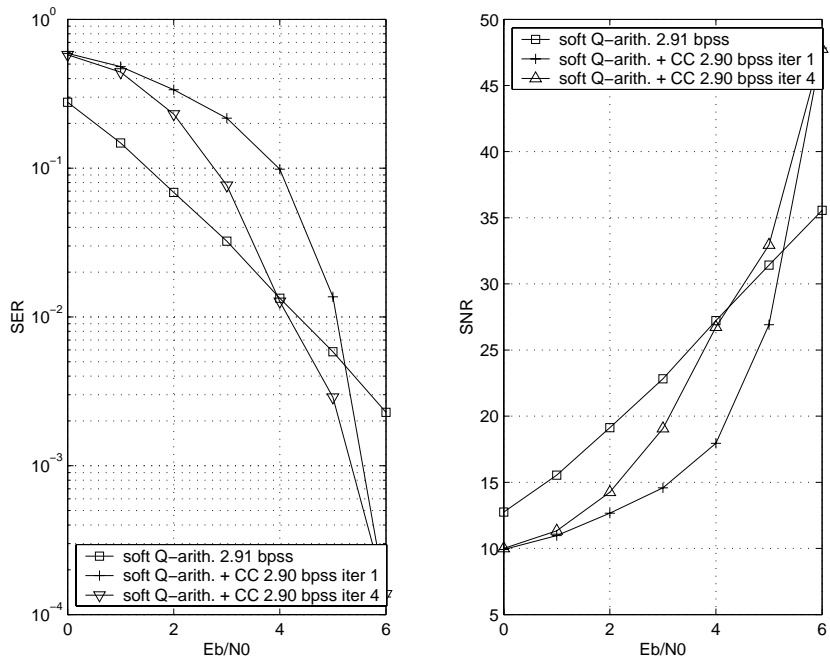


Figure 15: SER and SNR performances of (a) soft quasi-arithmetic decoding with soft synchronization (b) turbo quasi-arithmetic/channel decoding ($\rho = 0.5$, 200 symbols, 3000 channel realizations).

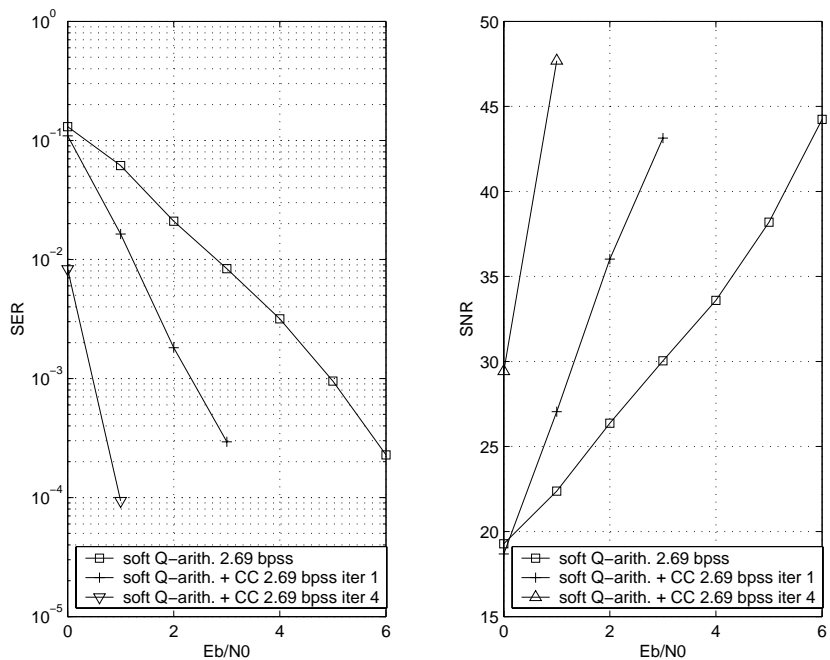


Figure 16: SER and SNR performances of (a) soft quasi-arithmetic decoding with soft synchronization (b) turbo quasi-arithmetic/channel decoding ($\rho = 0.9$, 200 symbols, 3000 channel realizations).

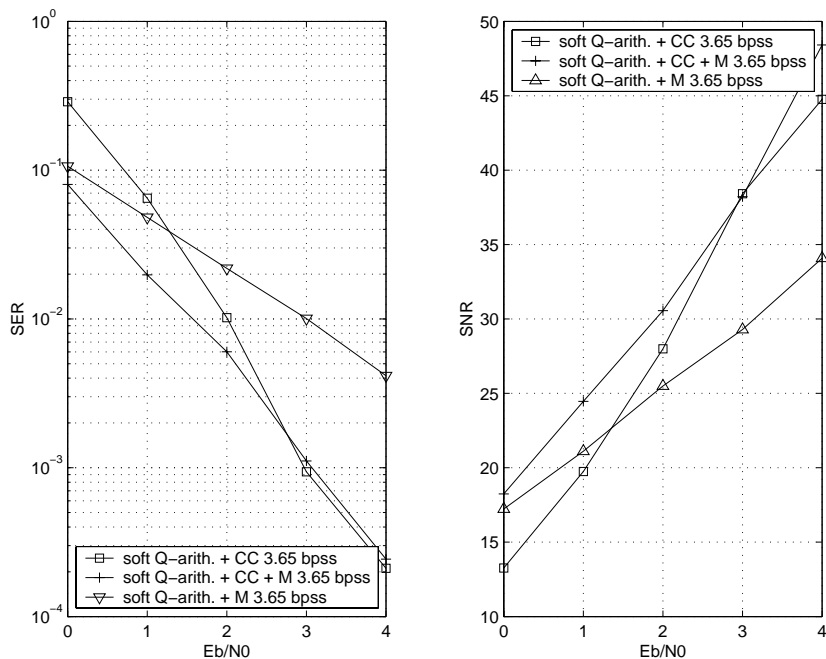


Figure 17: SER and SNR performances of (a) turbo quasi-arithmetic/channel decoding (b) turbo quasi-arithmetic/channel decoding with soft synchronization (c) soft quasi-arithmetic decoding with soft synchronization ($\rho = 0.5$, 200 symbols, 1500 channel realizations).

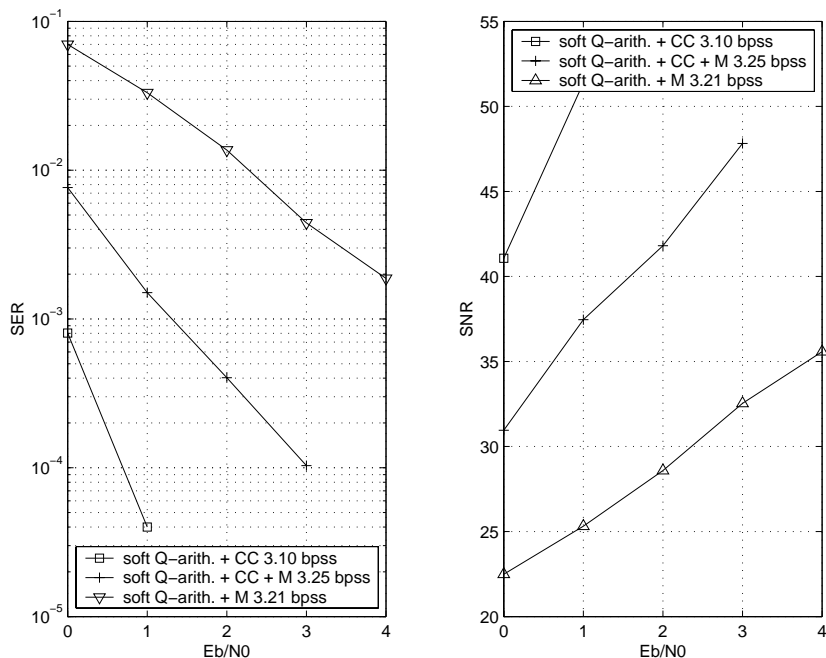


Figure 18: SER and SNR performances of (a) turbo quasi-arithmetic/channel decoding (b) turbo quasi-arithmetic/channel decoding with soft synchronization (c) soft quasi-arithmetic decoding with soft synchronization ($\rho = 0.9$, 200 symbols, 1500 channel realizations).

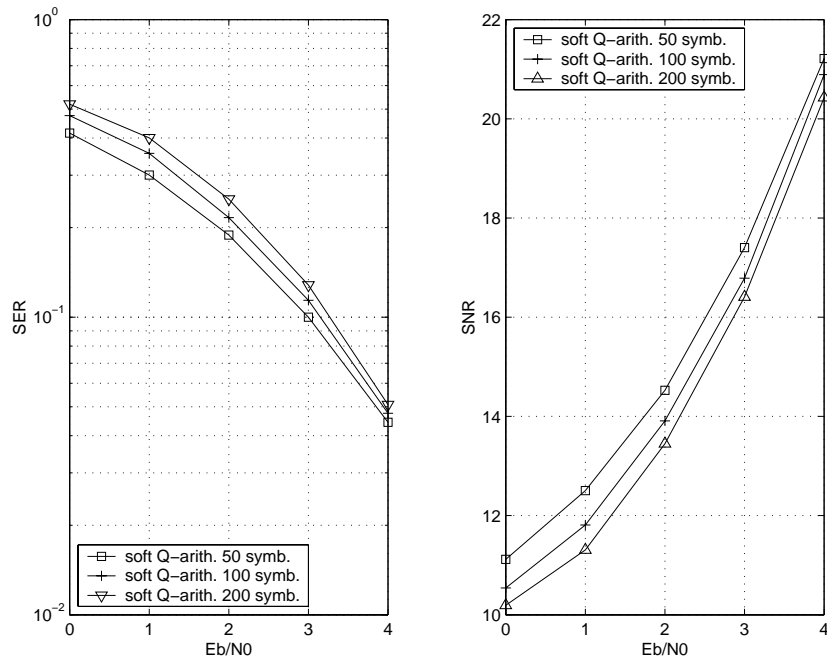


Figure 19: SER and SNR performances of soft quasi-arithmetic decoding for respectively 50, 100 and 200 symbols ($\rho = 0.5$, 3000 channel realizations).

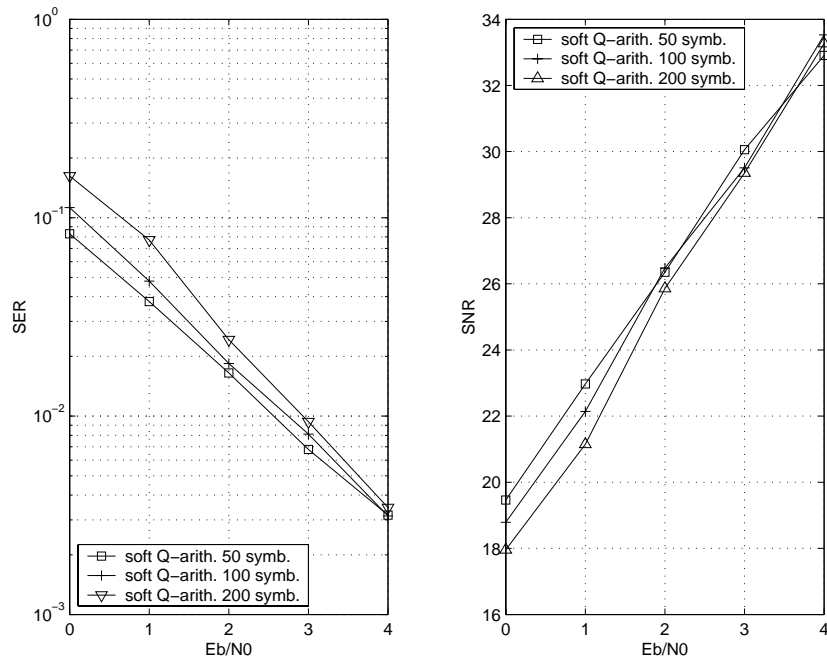


Figure 20: SER and SNR performances of soft quasi-arithmetic decoding for respectively 50, 100 and 200 symbols ($\rho = 0.9$, 3000 channel realizations).

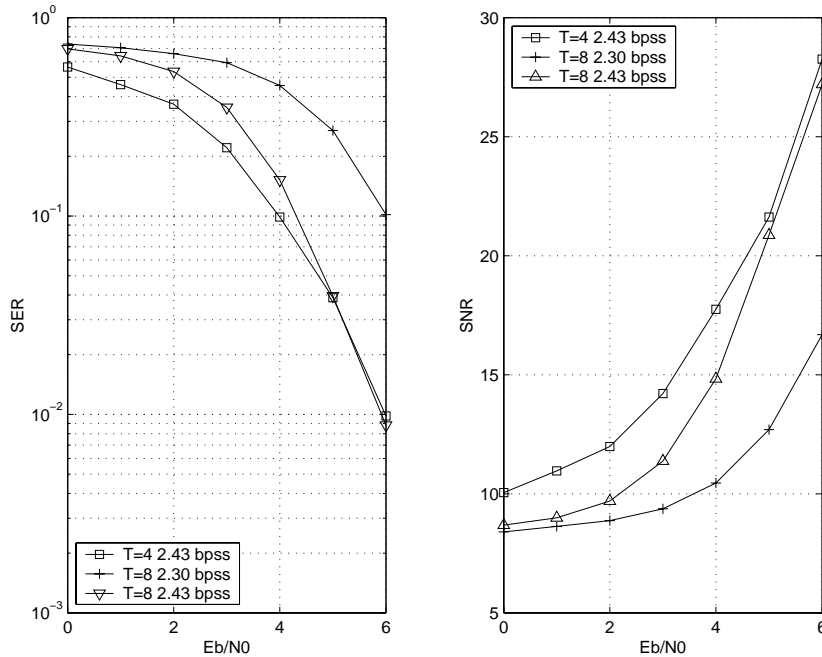


Figure 21: SER and SNR performances of (a) soft quasi-arithmetic decoding ($T = 4$) (b) soft quasi-arithmetic decoding ($T = 8$) (c) soft quasi-arithmetic decoding ($T = 8$) with soft synchronization ($\rho = 0.5$, 100 symbols, 3000 channel realizations).

11 Conclusion

Arithmetic codes are becoming more and more popular in practical compression systems and emerging standards. Their well-known drawback is however their very high sensitivity to noise. MAP estimators run on the coding tree can help to fight against errors and possible decoder de-synchronization but at the expense of rather high complexity. The coding tree grows exponentially with the number of symbols in the sequence to be coded. Here, we have considered an alternate solution based on reduced-precision arithmetic codes, called quasi-arithmetic codes. A quasi-arithmetic coder can be viewed as a finite state stochastic automaton. One can then run MAP estimators on the resulting model. For sake of clarity, in the examples we have considered simple source models. The results reported have been obtained considering an order-1 Markov source. However, the approach extends very easily to higher-order source models. The state model of the coding and decoding process is of finite size. Its size depends on the acceptable approximation of the source distribution. The decoding complexity remains within a realistic range without the need for applying any pruning. Placed in an iterative decoding structure in the spirit of serially concatenated turbo codes, the estimation process can then benefit from the iterations. Overall, the flexibility they offer for adjusting compression efficiency, complexity and error resilience, allows an optimal adaptation to various transmission conditions and terminal capabilities. Notice that, for low complexity, a very good trade-off compression - noise resilience can be achieved with quasi-arithmetic codes for low correlation sources. This emphasizes the interest of the above solution for practical systems, where the coder is applied on quantized de-correlated sequences of symbols.

References

- [1] L. R. Bahl, J. Cocke, F. Jelinek, and J. Raviv. Optimal decoding of linear codes for minimizing symbol error rate. *IEEE trans. on information theory*, 20:284–287, March 1974.
- [2] R. Bauer and J. Hagenauer. Iterative source/channel decoding based on a trellis representation for variable length codes. In *Proc. IEEE Intl. Symposium on Information Theory, ISIT*, page 117, June 2000.
- [3] R. Bauer and J. Hagenauer. Turbo fec/vlc decoding and its application to text compression. In *Proc. Conference on Information Theory and System*, pages WA6.6–WA6.11, March 2000.
- [4] C. Boyd, J. G. Cleary, S. A. Irvine, I. Rinsma-Melchert, and I. H. Witten. Integrating error detection into arithmetic coding. *IEEE trans. on Communications*, 45(1):1–3, Jan. 1997.
- [5] J. Chou and K. Ramchandran. Arithmetic coding-based continuous error detection for efficient arq-based image transmission. *IEEE Journal on Selected Areas in Communication*, 18(6):861–867, June 2000.
- [6] N. Demir and K. Sayood. Joint source-channel coding for variable length codes. In *Proc. IEEE Data Compression Conference, DCC*, pages 139–148, March 1998.
- [7] C. Demiroglu, M. W. Hoffman, and K. Sayood. Joint source channel coding using arithmetic codes and trellis coded modulation. In *Data Compression Conference*, Snowbird, UT, March 2001.
- [8] G. F. Elmasry. Embedding channel coding in arithmetic coding. *IEE proc.-Communications*, 146(2):73–78, April 1999.
- [9] G. F. Elmasry. Joint lossless-source and channel coding using automatic repeat request. *IEEE trans. on Communications*, 47(7):953–955, July 1999.
- [10] T. Guionnet and C. Guillemot. Soft decoding and synchronization of arithmetic codes : application to image transmission over error-prone channels. *Submitted to IEEE trans. on Image Processing*, 2002.
- [11] A. Guyader, E. Fabre, C. Guillemot, and M. Robert. Joint source-channel turbo decoding of entropy coded sources. *IEEE Journal on Selected Areas in Communication, special issue on the turbo principle : from theory to practice*, 19(9):1680–1696, September 2001.
- [12] P. G. Howard and J. S. Vitter. *Image and Text Compression*, pages 85–112. Kluwer Academic Publisher, 1992.
- [13] P. G. Howard and J. S. Vitter. Design and analysis of fast text compression based on quasi-arithmetic coding. In *Data Compression Conference*, pages 98–107, Snowbird, Utah, March-April 1993.
- [14] I. Kozintsev, J. Chou, and K. Ramchandran. Image transmission using arithmetic coding based continuous error detection. In *Data Compression Conference*, pages 339–348, Snowbird, UT, March 1998.

- [15] A.H. Murad and T.E. Fuja. Joint source-channel decoding of variable length encoded sources. In *Proc. Information Theory Workshop, ITW*, pages 94–95, June 1998.
- [16] M. Park and D. J. Miller. Joint source-channel decoding for variable-length encoded data by exact and approximate map sequence estimation. *IEEE Trans. on Communications*, 48(1):1–6, January 2000.
- [17] M. Park and D.J. Miller. Decoding entropy-coded symbols over noisy channels by MAP sequence estimation for asynchronous HMMs. In *Proc. Conf. on Info. Sciences and Systems*, May 1998.
- [18] R. Pasco. *Source coding algorithms for fast data compression*. PhD thesis, Dept. of Electrical Engineering, Stanford Univ., Stanford Calif., 1976.
- [19] B. D. Pettijohn, M. W. Hoffman, and K. Sayood. Joint source/channel coding using arithmetic codes. *IEEE trans. on Communications*, 49(5):826–836, May 2001.
- [20] J. J. Rissanen. Generalized kraft inequality and arithmetic coding. *IBM J. Res. Develop.*, 20:198–203, May 1976.
- [21] J. J. Rissanen. Arithmetic codings as number representations. *Acta Polytech. Scand. Math.*, 31:44–51, Dec. 1979.
- [22] I. Sodagar, B. B. Chai, and J. Wus. A new error resilience technique for image compression using arithmetic coding. In *IEEE International Conference on Accoustics, Speech and Signal Processing*, Istanbul, Turkey, June 2000.
- [23] K. P. Subbalakshmi and J. Vaisey. On the joint source-channel decoding of variable-length encoded sources: The bsc case. *IEEE trans. on Communications*, 49(12):2052–2055, December 2001.
- [24] J. Wen and J. D. Villasenor. Reversible variable length codes for efficient and robust image and video coding. In *Proc. IEEE Data Compression Conference, DCC*, pages 471–480, April 1998.
- [25] I. H. Witten, R. M. Neal, and J. G. Cleary. Arithmetic coding for data compression. *Communications of the ACM*, 30(6):520–540, June 1987.
- [26] M. Wada Y. Takishima and H. Murakami. Reversible variable length codes. *IEEE Trans. on Communications*, 43(4):158–162, April 1995.